Supporting Information

Modulating magnetic dynamics through tailoring the terminal ligands in Dy2 single–molecule magnets

Peipei Cen,[a,c] Xiangyu Liu,[b,c*] Yi-Quan Zhang,[d*] Jesús Ferrando-Soria,[c] Gang Xie,[a] Sanping Chen,[a*] and Emilio Pardo[c]

[a] Key Laboratory of Synthetic and Natural Functional Molecule Chemistry of Ministry of Education, College of Chemistry and Materials Science, Northwest University, Xi'an 710069, China

[b] State Key Laboratory of High-efficiency Utilization of Coal and Green Chemical Engineering, National Demonstration Center for Experimental Chemistry Education, College of Chemistry and Chemical Engineering, Ningxia University, Yinchuan 750021, China

[c] Departamento de Química Inorgánica, Instituto de Ciencia Molecular (ICMOL), Universidad de Valencia, Paterna 46980, Valencia, Spain.

[d] Jiangsu Key Laboratory for NSLSCS, School of Physical Science and Technology, Nanjing Normal University, Nanjing 210023, China

***Corresponding author**

Prof. Sanping Chen

E-mail: sanpingchen@126.com

***Corresponding author**

Dr. Xiangyu Liu

E-mail: xiangyuliu432@126.com

***Corresponding author**

Dr. Yi-Quan Zhang

E-mail: zhangyiquan@njnu.edu.cn

Table of contents

Table S1. Crystal data and structure refinement details for **1** and **2**.

compound	**1**	**2**
Empirical formula	$C_{64}H_{42}ClDy_2F_{12}N_8O_{10}$	$C_{56}H_{34}Dy_2F_{12}N_8O_{10}S_4$
Formula weight	1636.06	1660.19
Crystal system	triclinic	trigonal
Space group	*P*-1	$P3_1$
a / (Å)	13.5287(6)	13.6044(4)
b / (Å)	13.9447(6)	13.6044(4)
c / (Å)	18.7450(8)	28.6443(8)
α / (°)	93.001(4)	90
β / (°)	100.392(4)	90
γ / (°)	116.780(4)	120
V (Å^3)	3069.1(3)	4591.2(3)
Z	2	3
D_c / (g cm^{-3})	1.770	1.801
Absorption coeff.(μ)mm^{-1}	2.519	15.077
F(000)	1604.0	2430.0
R(int)	0.0639	0.0457
Θ range / (°)	2.234 to 50.02	7.504 to 131.858
Reflections collected / unique	14960	9825
Parameters refined	867	844
Final *R* indices [I>2σ(I)]	R_1 = 0.1329, wR_2 = 0.3205	R_1=0.0417,wR_2 = 0.1022
R indices (all data)	R_1 = 0.1585, wR_2 = 0.3479	R_1=0.0453,wR_2 = 0.1058
Temp.(K)	100(2)	150.00(10)

Table S2. Selected bond lengths (Å) and bond angles (°) for **1** and **2**.

1					
Dy(1)-O(3)	2.34(2)	N(5)-C(30)	1.28(4)	O(3)-Dy(1)-N(6)	68.13(15)
Dy(1)-O(1)	2.37(2)	N(4)-C(44)	1.34(4)	O(4)-Dy(1)-N(6)	71.86(16)
Dy(1)-O(4)	2.34(2)	C(1)-C(39)	1.40(6)	O(1)-Dy(1)-N(6)	74.1(7)
Dy(1)-O(5)	2.376(19)	O(3)-Dy(1)-O(4)	70.6(7)	O(5)-Dy(1)-N(6)	65.4(7)
Dy(1)-O(2)	2.38(2)	O(3)-Dy(1)-O(1)	147.7(7)	O(2)-Dy(1)-N(6)	139.7(7)
Dy(1)-O(6)	2.45(2)	O(4)-Dy(1)-O(1)	95.4(7)	O(6)-Dy(1)-N(6)	117.1(7)
Dy(1)-N(2)	2.52(3)	O(3)-Dy(1)-O(5)	84.9(7)	N(2)-Dy(1)-N(6)	147.7(8)
Dy(1)-N(6)	2.67(2)	O(4)-Dy(1)-O(5)	136.1(7)	O(3)-Dy(1)-N(1)	116.7(8)
Dy(1)-N(1)	2.69(3)	O(1)-Dy(1)-O(5)	86.3(7)	O(4)-Dy(1)-N(1)	62.1(8)
Dy(2)-O(6)	2.32(2)	O(3)-Dy(1)-O(2)	139.8(7)	O(1)-Dy(1)-N(1)	78.0(8)
Dy(2)-O(10)	2.35(2)	O(4)-Dy(1)-O(2)	130.0(7)	O(5)-Dy(1)-N(1)	157.7(8)

Dy(2)-O(7)	2.350(19)	O(1)-Dy(1)-O(2)	71.5(7)	O(2)-Dy(1)-N(1)	68.0(8)
Dy(2)-O(8)	2.36(2)	O(5)-Dy(1)-O(2)	92.1(7)	O(6)-Dy(1)-N(1)	118.2(7)
Dy(2)-O(9)	2.38(2)	O(3)-Dy(1)-O(6)	69.8(7)	O(5)-Dy(1)-O(6)	61.8(6)
Dy(2)-O(5)	2.403(19)	O(4)-Dy(1)-O(6)	133.5(7)	O(2)-Dy(1)-O(6)	73.6(7)
Dy(2)-N(5)	2.49(3)	O(1)-Dy(1)-O(6)	131.0(7)	O(6)-Dy(2)-O(10)	87.4(7)
			2		
Dy(1)-O(2)	2.350(6)	O(2)-Dy(1)-O(4)	132.6(2)	O(10)-Dy(2)-N(5)	78.7(3)
Dy(1)-O(4)	2.367(7)	O(1)-Dy(1)-O(2)	72.4(3)	O(7)-Dy(2)-O(10)	143.4(2)
Dy(1)-O(6)	2.412(6)	O(4-Dy(1)-O(6)	119.5(6)	O(7)-Dy(2)-O(5)	75.1(2)
Dy(1)-O(1)	2.330(6)	O(3)-Dy(1)-O(4)	70.3(2)	O(7)-Dy(2)-N(4)	66.8(3)
Dy(1)-O(3)	2.364(7)	N(2)-Dy(1)-N(1)	62.0(3)	O(8)-Dy(2)-O(4)	142.7(3)
Dy(1)-O(5)	2.359(6)	O(2)-Dy(1)-N(2)	72.4(3)	O(8)-Dy(2)-O(6)	84.5(3)
Dy(1)-N(2)	2.501(9)	O(1)-Dy(1)-N(2)	132.6(3)	O(7)-Dy(2)-O(6)	88.9(2)
Dy(1)-N(6)	2.600(8)	O(4)-Dy(1)-N(2)	116.0(8)	O(7)-Dy(2)-N(3)	132.7(3)
Dy(2)-O(10)	2.392(7)	O(3)-Dy(1)-N(2)	75.4(3)	O(7)-Dy(2)-N(5)	74.7(3)
Dy(2)-O(8)	2.319(7)	C(5)-O(2)-Dy(1)	136.5(6)	O(8)-Dy(2)-O(7)	72.3(3)
Dy(2)-O(5)	2.434(6)	O(9)-Dy(2)-O(8)	92.5(3)	O(8)-Dy(2)-O(5)	134.5(3)
Dy(1)-N(1)	2.650(10)	O(9)-Dy(2)-O(5)	133.0(2)	O(8)-Dy(2)-N(3)	67.1(3)
Dy(2)-O(9)	2.302(7)	O(9)-Dy(2)-N(4)	64.3(3)	O(8)-Dy(2)-N(5)	134.9(3)
Dy(2)-O(7)	2.338(7)	O(10)-Dy(2)-O(5)	70.1(2)	O(6)-Dy(2)-O(5)	63.8(2)
Dy(2)-O(6)	2.353(6)	O(10)-Dy(2)-N(4)	120.5(2)	O(6)-Dy(2)-N(4)	153.0(2)
Dy(2)-N(3)	2.588(9)	O(9)-Dy(2)-O(6)	137.2(2)	O(5)-Dy(2)-N(3)	119.0(2)
Dy(2)-N(4)	2.686(9)	O(9)-Dy(2)-N(3)	75.1(3)	O(8)-Dy(2)-N(4)	77.3(3)
Dy(2)-N(5)	2.505(8)	O(9)-Dy(2)-N(5)	86.3(3)	O(6)-Dy(2)-O(10)	86.0(2)
S(1)-C(1)	1.652(9)	O(10)-Dy(2)-N(3)	76.3(3)	O(6)-Dy(2)-N(3)	64.5(2)

Table S3. Dy^{III} ion geometry analysis of **1** and **2** by SHAPE 2.1 software.

Configuration	ABOXIY, 1		ABOXIY, 2	
	Dy(1)	Dy(2)	Dy(1)	Dy(2)
Heptagonal bipyramid (D_{7h})	17.476	17.078	17.202	17.158
Johnson triangular cupola J3 (C_{3v})	15.405	15.063	15.802	14.946
Capped cube J8 (C_{4v})	8.539	8.289	8.468	8.890
Spherical-relaxed capped cube (C_{4v})	7.714	7.363	7.341	7.808
Capped square antiprism J10 (C_{4v})	3.025	2.850	2.749	2.917
Spherical capped square antiprism (C_{4v})	2.365	2.233	2.205	2.261

Tricapped trigonal prism J51 (D_{3h})	2.412	2.163	2.466	2.222
Spherical tricapped trigonal prism (D_{3h})	2.579	1.928	2.291	2.303
Tridiminished icosahedron J63 (C_{3v})	10.463	11.587	11.095	10.412
Hula-hoop (C_{2v})	7.512	8.177	7.410	7.901
Muffin (C_s)	2.268	2.120	1.779	2.235

Table S4. Relaxation fitting parameters from least-squares fitting of $\chi(f)$ data under 0 dc field of **1.**

T(K)	χ_T	χ_S	α
2	9.845	0.422	0.149
3	7.437	0.402	0.125
4	5.896	0.392	0.086
4.2	5.574	0.361	0.085
4.5	5.191	0.352	0.068
4.8	4.893	0.354	0.053
5	4.726	0.360	0.046
5.2	4.552	0.343	0.041
5.5	4.341	0.341	0.033
5.8	4.152	0.353	0.028
6	4.024	0.368	0.020
6.5	3.753	0.401	0.017
7	3.526	0.391	0.031
7.5	3.324	0.892	0.010
8	3.138	1.067	0.015
14.5	0.330	0.025	0.025
15	0.320	0.018	0.023
15.5	0.309	0.024	0.024
16	0.300	0.021	0.018
16.5	0.291	0.019	0.016
17	0.284	0.011	0.010
17.5	0.276	0.011	0.009
18	0.270	0.005	0.021
18.5	0.263	0.002	0.028

Table S5. Relaxation fitting parameters from least-squares fitting of $\chi(f)$ data under 1200 Oe dc field of **1**.

T(K)	χ_T	χ_S	α
2	13.788	3.152	0.333
3	10.442	2.364	0.205
4	8.641	1.915	0.100
4.2	8.356	1.840	0.087
4.5	7.948	1.739	0.071
4.8	7.561	1.643	0.061
5	7.335	1.600	0.052
5.2	7.114	1.542	0.049
5.5	6.816	1.478	0.042
5.8	6.541	1.429	0.036
6	6.351	1.408	0.030
6.5	5.963	1.359	0.027
7	5.617	1.154	0.022
7.5	5.324	0.297	0.043
8	5.038	0.535	0.084

Table S6. Relaxation fitting parameters from least-squares fitting of $\chi(f)$ data under 1200 Oe dc field of **2**.

T(K)	χ_T	χ_S	α
2	4.220	1.642	0.253
2.5	3.716	1.384	0.206
3	3.330	1.226	0.170
3.2	3.193	1.194	0.154
3.5	2.992	1.183	0.120
3.8	2.837	1.052	0.133
4	2.730	1.009	0.126
4.5	2.494	0.877	0.115
5	2.291	0.694	0.108
5.5	2.116	0.279	0.102

Table S7. Calculated energy levels (cm^{-1}), g (g_x, g_y, g_z) tensors and m_J values of the lowest eight Kramers doublets (KDs) of individual Dy^{III} fragments of complex **1** using CASSCF/RASSI with MOLCAS 8.2.

	1(Dy1)			**1**(Dy2)		
	E/cm^{-1}	g	m_J	E/cm^{-1}	g	m_J
1	0.0	0.226 0.309 19.574	±15/2	0.0	0.032 0.047 19.741	±15/2
2	61.6	1.099 1.446 16.943	±5/2	132.8	0.312 0.647 16.219	±13/2
3	104.2	1.060 2.148 13.742	±13/2	191.6	2.449 3.083 12.443	±7/2
4	144.2	4.758 6.829 9.451	±11/2	233.4	8.076 6.527 2.441	±11/2
5	192.4	0.228 2.762 13.830	±7/2	285.8	0.255 3.938 13.452	±5/2
6	233.4	0.566 3.505 12.275	±9/2	314.8	1.810 4.522 11.192	±9/2
7	294.5	0.371 2.667 13.533	±3/2	385.6	0.171 2.787 13.858	±3/2
8	324.1	0.802 2.361 16.258	±1/2	419.3	0.765 2.345 16.627	±1/2

Table S8. Calculated energy levels (cm^{-1}), g (g_x, g_y, g_z) tensors and m_J values of the lowest eight Kramers doublets (KDs) of individual Dy^{III} fragments of complex **2** using CASSCF/RASSI with MOLCAS 8.2.

	2(Dy1)			**2**(Dy2)		
	E/cm^{-1}	g	m_J	E/cm^{-1}	g	m_J
1	0.0	0.072 0.097 19.713	±15/2	0.0	0.075 0.128 19.670	±15/2
2	100.0	2.579 5.648 13.066	±13/2	111.2	1.180 3.007 14.810	±13/2
3	128.3	9.661 5.214 0.216	±3/2	151.9	4.475 5.056 11.823	±11/2

4	166.0	3.052 4.868 10.702	±11/2	171.3	0.155 1.516 13.378	±1/2
5	230.9	0.281 2.031 14.719	±5/2	239.9	0.482 1.448 14.683	±9/2
6	270.1	1.375 2.549 13.205	±9/2	286.7	2.693 4.391 10.383	±7/2
7	317.1	1.783 2.565 14.876	±7/2	327.7	3.180 3.959 10.949	±5/2
8	378.2	0.415 0.606 18.192	±1/2	370.7	0.796 1.721 16.546	±3/2

Table S9. Wave functions with definite projection of the total moment | m_J > for the lowest two KDs of individual Dy^{III} fragments for **1** and **2** using CASSCF/RASSI-SO with MOLCAS 8.2.

<table>
<tr><th></th><th>E/cm^{−1}</th><th>wave functions</th></tr>
<tr><td rowspan="2">1_Dy1</td><td>0.0</td><td>97%|±15/2></td></tr>
<tr><td>61.6</td><td>10%|±7/2>+18%|±5/2>+23%|±3/2>+30%|±1/2></td></tr>
<tr><td rowspan="2">1_Dy2</td><td>0.0</td><td>98%|±15/2></td></tr>
<tr><td>132.8</td><td>84%|±13/2></td></tr>
<tr><td rowspan="2">2_Dy1</td><td>0.0</td><td>98%|±15/2></td></tr>
<tr><td>100.0</td><td>64%|±13/2>+12%|±11/2>+12%|±1/2></td></tr>
<tr><td rowspan="2">2_Dy2</td><td>0.0</td><td>97%|±15/2></td></tr>
<tr><td>111.2</td><td>75%|±13/2>+12%|±9/2></td></tr>
</table>

Table S10. Natural Bond Order (NBO) charges per atoms in the ground state of complexes **1** and **2** using CASSCF/RASSCI with MOLCAS 8.2.

	1(Dy1)	**1(Dy2)**	**2(Dy1)**	**2(Dy2)**
Dy	2.5189	2.5198	2.5183	2.5166
Lu	1.4795	1.4488	1.4490	1.4426
O1	−0.7144	−0.7062	−0.7192	−0.7353
O2	−0.6395	−0.7005	−0.7037	−0.6869
O3	−0.6945	−0.7468	−0.6809	−0.6824
O4	−0.7427	−0.7057	−0.7440	−0.7198
O5	−0.7649	−0.7356	−0.7312	−0.7172
O6	−0.7234	−0.7344	−0.6980	−0.7179
N1	−0.2341	−0.2145	−0.2295	−0.2355
N2	−0.3076	−0.3308	−0.3061	−0.3171
N3	−0.3174	−0.3270	−0.3189	−0.3327

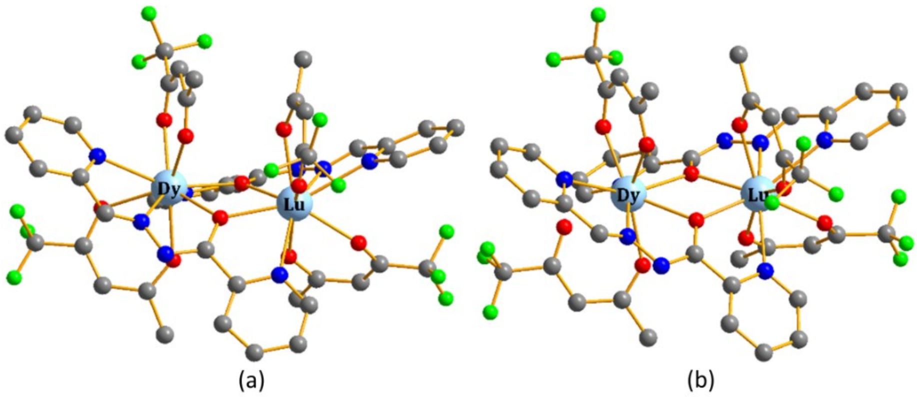

Figure S1. Calculated model structures of individual Dy^{III} fragments of complexes **1**−**2**; H atoms are omitted

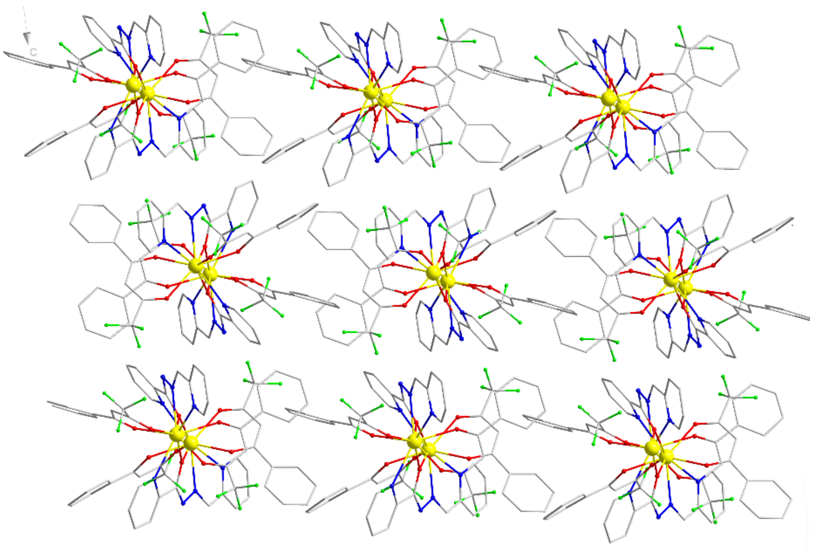

Figure S2. Molecular stacking chart of **1**.

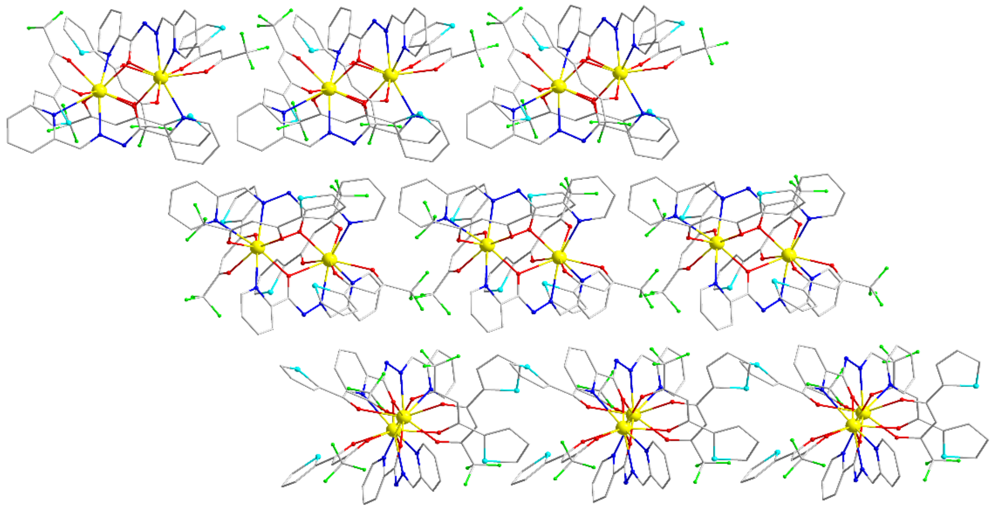

Figure S3. Molecular stacking chart of **2**.

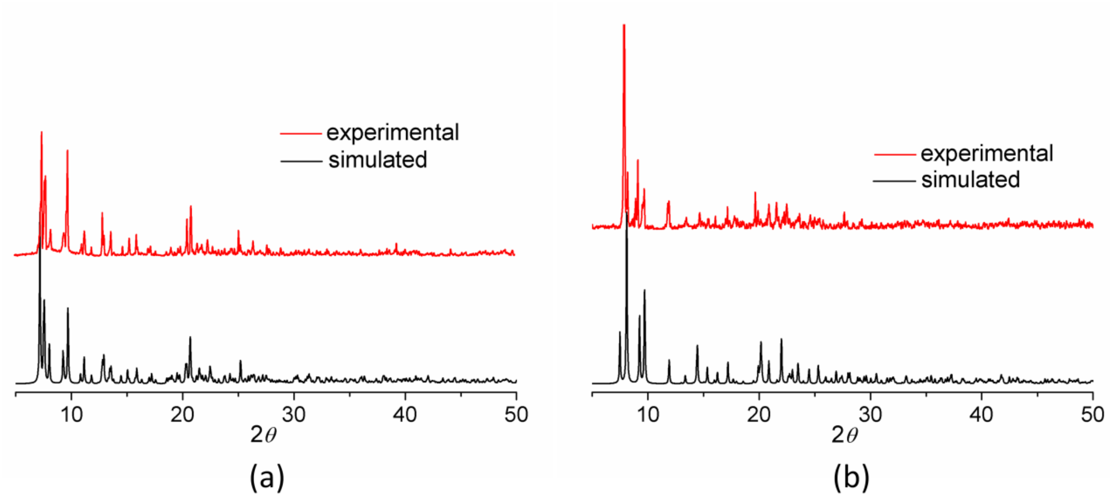

Figure S4. PXRD curves of **1** (a) and **2** (b)

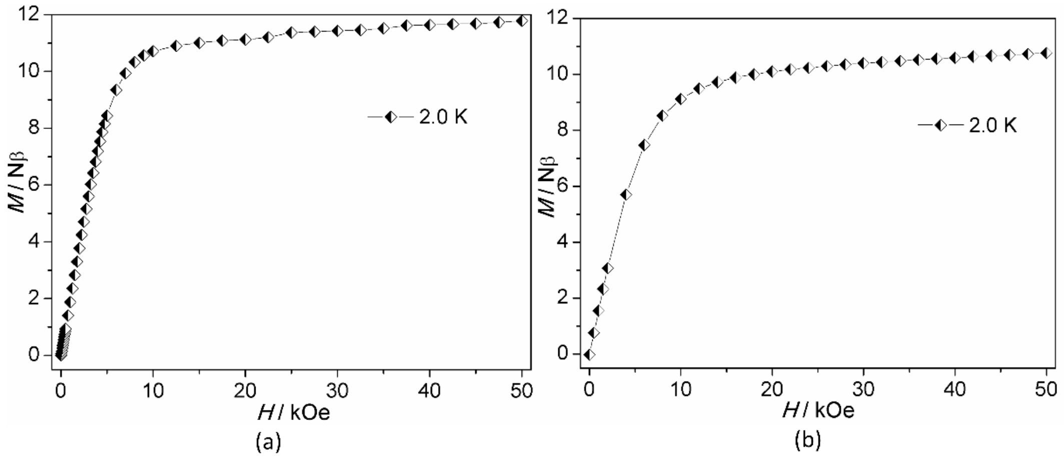

Figure S5. *M* vs *H* curves for compounds **1** (a) and **2** (b) at 2 K.

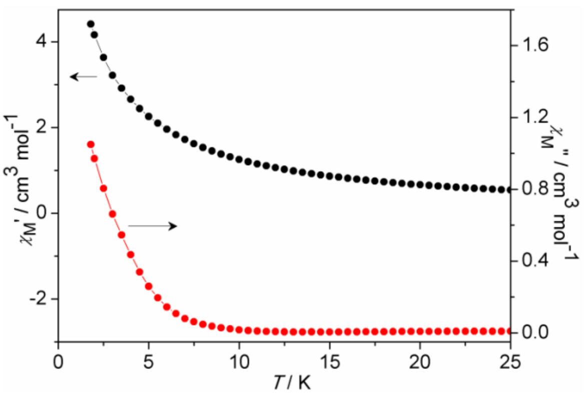

Figure S6. Temperature dependence of the in-phase (χ') and out-of-phase (χ'') of the ac susceptibilities for **2** under zero dc field.

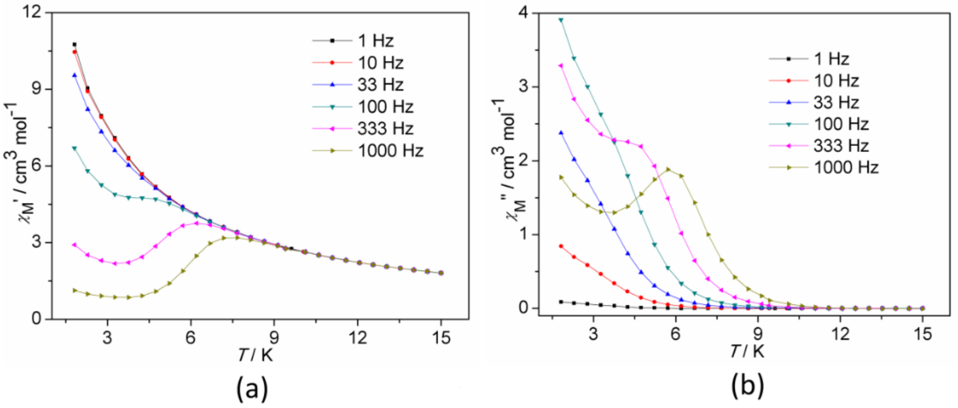

Figure S7. Temperature dependence of the in-phase (χ') and out-of-phase (χ'') ac susceptibilities for **1** under zero dc field.

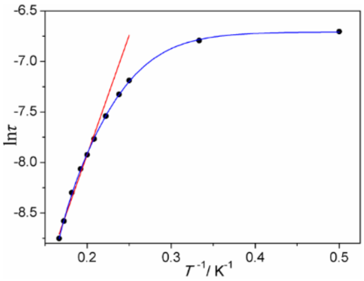

Figure S8. Plot of relaxation time (ln τ) vs T^{-1} for complexes **1** at zero dc field. The red lines and blue lines represent the Arrhenius fit and multiple relaxation processes, respectively.

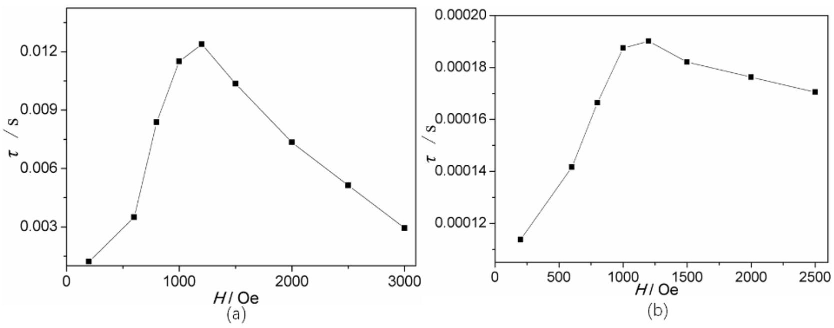

Figure S9. Field dependence of the magnetic relaxation time at 2 K for **1** (a) and **2** (b).

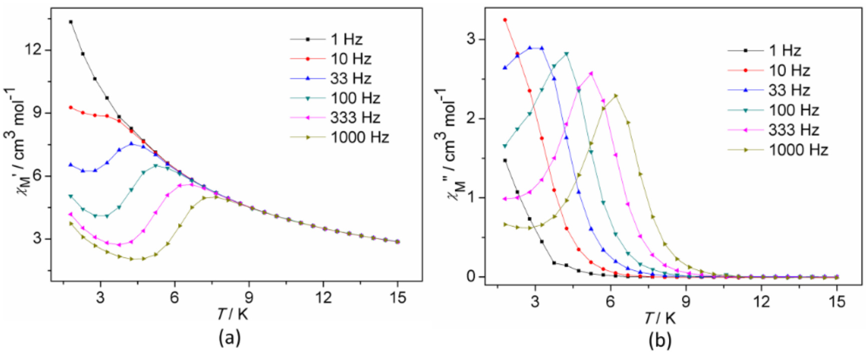

Figure S10. Temperature dependence of in-phase (χ') and out-of-phase (χ'') ac susceptibilities for **1** at applied dc fields of 1200 Oe.

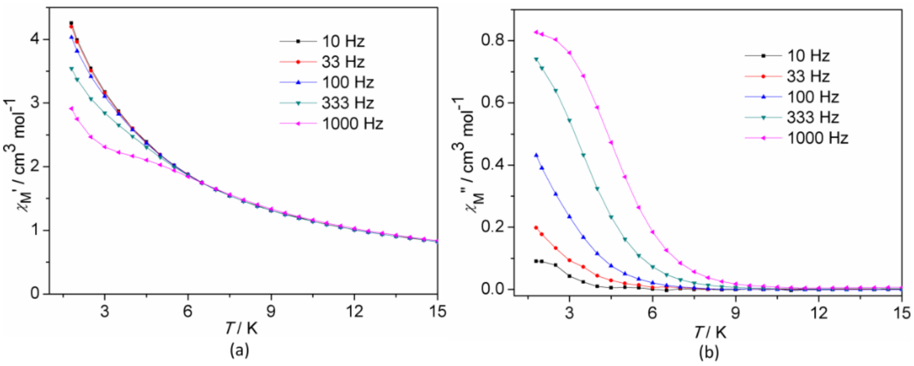

Figure S11. Temperature dependence of in-phase (χ') and out-of-phase (χ'') ac susceptibilities for **2** at applied dc fields of 1200 Oe

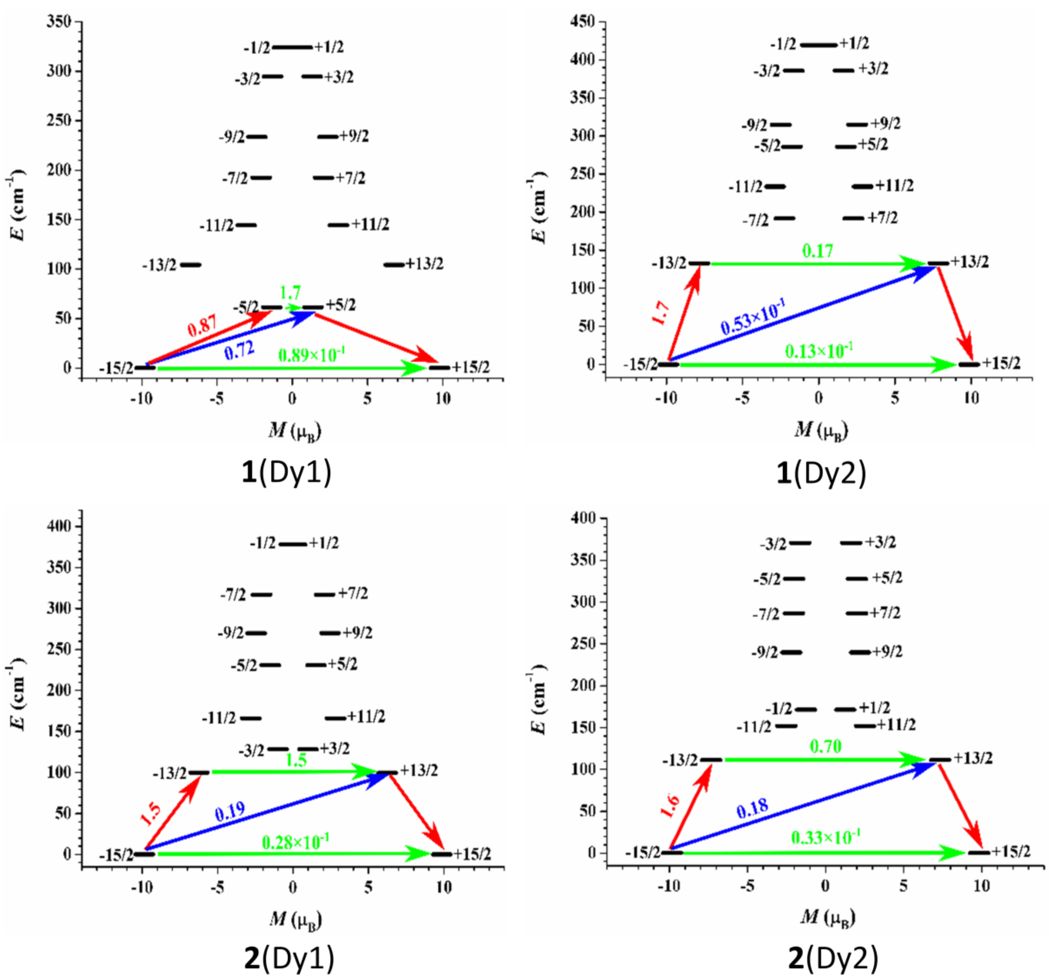

Figure S12. Magnetization blocking barriers for individual Dy^{III} fragments in complexes **1** (top) and **2** (bottom). The thick black lines represent the KDs as a function of their magnetic moment along the magnetic axis. The green lines correspond to the diagonal matrix element of the transversal magnetic moment; the blue lines represent Orbach relaxation processes. The path shown by the red arrows represents the most probable path for magnetic relaxation in the corresponding compounds. The numbers at each arrow stand for the mean absolute value of the corresponding matrix element of transition magnetic moment.

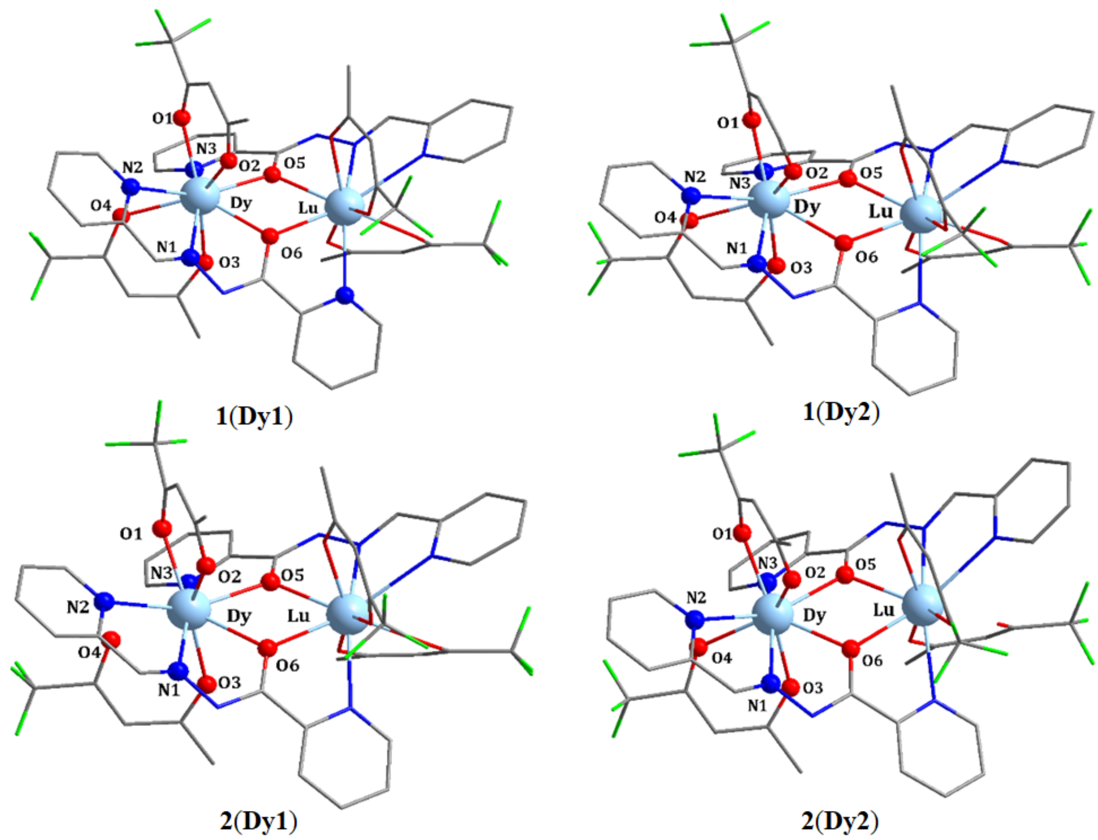

Figure S13. Labeled molecular structure of complexes **1** and **2**.